Journal of Sulfur Chemistry
Publication details, including instructions for authors and subscription information:
http://www.informaworld.com/smpp/title~content=t713926081

Reactivity of disulfide peptide l-cystine with iodido (diethylenetriamine)platinum(II) and synthesis of products in the presence of an iodide ion

Trilochan Swain[a]; Prakash Mohanty[b]
[a] Faculty of Chemistry, Indic Institute of Design and Research, Bhubaneswar, Orissa, India [b] Department of Chemistry, Utkal University, Bhubaneswar, Orissa, India

First published on: 22 October 2010

To cite this Article Swain, Trilochan and Mohanty, Prakash(2010) 'Reactivity of disulfide peptide l-cystine with iodido (diethylenetriamine)platinum(II) and synthesis of products in the presence of an iodide ion', Journal of Sulfur Chemistry, 31: 6, 533 — 544, First published on: 22 October 2010 (iFirst)
To link to this Article: DOI: 10.1080/17415993.2010.525708
URL: http://dx.doi.org/10.1080/17415993.2010.525708

Journal of Sulfur Chemistry
Vol. 31, No. 6, December 2010, 533–544

Taylor & Francis
Taylor & Francis Group

Reactivity of disulfide peptide L-cystine with iodido (diethylenetriamine)platinum(II) and synthesis of products in the presence of an iodide ion

Trilochan Swain[a]* and Prakash Mohanty[b]

[a]*Faculty of Chemistry, Indic Institute of Design and Research, Bhubaneswar, Orissa, India;* [b]*Department of Chemistry, Utkal University, Bhubaneswar-751004, Orissa, India*

(*Received 2 August 2010; final version received 18 September 2010*)

Substitution reactions of complex $[PtI(dien)]^+$ (where, dien = diethylenetriamine) with sulfur-containing peptide L-cystine has been studied in 1.0×10^{-1} M aqueous perchlorate or acetate medium between $298 \leq T\,(K) \leq 323$ and $2.30 \leq pH \leq 4.45$ using a UV–visible spectrophotometer. Products obtained have characterized from their physico-chemical and spectroscopic methods at various pH and temperatures. From this characterization, products have indicated that $[PtI(dien)]^+$ has formed a complex with L-cystine and acts as a bidentate ligand, through Pt–S bond at $2.30 \leq pH \leq 3.30$ and through Pt–N and Pt–S bond of cystine in $3.95 \leq pH \leq 4.45$. At $2.30 \leq pH \leq 3.30$, ring opening and closing of dien have occurred at 308 and 323 K, respectively, and the same has happened at $pH \geq 3.95$. All reactions have followed the rate law $-\,d[mixture]/dt = (k_1 + k_2[cystine])\,[Pt(II)]$, where k_2 denotes the second-order rate constant. Activation parameters E_a, $\Delta H^{\#}$ and $\Delta S^{\#}$ have been determined. Product formation and reversible and forward reaction rate constants have also been evaluated.

Keywords: $[PtI(dien)]^+$; L-cystine; kinetics; mechanism; ^1H NMR data sets; IR

1. Introduction

It is believed that part of the nephrotoxicity, gastrointestinal toxicity, neurotoxicity, ototoxicity, drug resistance (*1*, *2*) and possible bone marrow suppression may involve the reaction of Pt(II) with sulfur-containing compounds with the subsequent inactivation of essential enzymes and other proteins (*3–6*). The biological and medicinal activities of platinum(II), *cis*-$Pt(NH_3)_2Cl_2$ have been governed by their complex chemical reactions with a variety of sulfur-containing biomolecules (*7–13*) such as 2-(3-amino propylamino)-ethylphosphorothioic acid (*14–16*), sodium thiosulfate (*16, 17*), sodium diethyldithiocarbamate (*18, 19*) and glutathione (GSH) (*20, 21*). These have acted as inhibitors of cisplatin nephrotoxicity (*14, 15*). The products of the reactions of $[\{trans\text{-}PtCl(NH_3)_2\}_2\text{-}\mu\text{-}\{trans\text{-}Pt(NH_3)_2(NH_2(CH_2)_6NH_2)_2\}](NO_3)_4$ (BBR3464;1,0,1/t,t,t, $n = 6$), $[\{trans\text{-}PtCl(NH_3)_2\}_2\text{-}\mu\text{-}(H_2N(CH_2)_6NH_2)](NO_3)_2$ (BBR3005;1,1/t,t, $n = 6$), $[\{trans\text{-}PtCl(NH_3)_2\}_2\text{-}\mu\text{-}(H_2N(CH_2)_4$

*Corresponding author. Email: scienceorissa@rediffmail.com

ISSN 1741-5993 print/ISSN 1741-6000 online

DOI: 10.1080/17415993.2010.525708
http://www.informaworld.com

NH_2)]Cl_3 (BBR3571;1,1/t,t-spermidine, $n = 3, 4$) and *trans*-[$PtCl_2(NH_3)_2$] (*t*-DDP) with sulfur-containing tripeptide-reduced GSH in phosphate-buffered saline have been characterized by NMR spectroscopy and HPLC (*22*). Recently, some Pt(II) complexes derived from biologically active sulfur donor ligands 1*H*-indol-2,3-dione benzothiazoline (Bzt_1H) and 5-nitro-1*H*-indol-2, 3-dione benzothiazoline (Bzt_2H) have been isolated for antimicrobial activity study (*23*). [PtX(dien)]X (X = Cl, Br, I) has no antitumor activity (*24, 25*) even though chemical reactivity with nucleic acid bases resembles *cis*-$Pt(NH_3)_2Cl_2$ (*25*) as an antitumor agent and both have provided substitution on Pt(II) center. The ligand substitution on coordination compounds of Pt(II) with tridentate and bidentate ligands such as diethylenetriamine (dien), bis(2-pyridylmethyl)amine (bpma), 2,2′:6′,2″-terpyridine (terpy) and ethylenediamine (en) has provided very useful substrates for studies of square planar complexes even at acidic pH (*26–28*). Using cystine as a nucleophile (*28*), some substitutions are reported with ene or diene ligand-coordinated square planar Pt(II). Kinetic studies on the oxidation of disulfide peptide L-cystine by potassium ferrate (*29a*), alkaline permanganate (*29b*), iodine, chlorite and chlorine dioxide (*29c*) and electrolytic oxidation of L-cystine at a carbon paste electrode modified with ruthenium(IV) oxide (*29d*) have been reported. A number of amino acids including this peptide, cystine, have been prepared with Fe(II) which apparently contain intact S−S bonds (*30*). This has prompted us to undertake the present work using the same peptide with $[PtI(dien)]^+$ complex in the presence of an iodide ion. However, to the best of our knowledge, this reaction of square planar Pt(II) complex in the presence of I^- investigated in this work has not yet been reported previously. The main objective was to determine the kinetic parameters and characterize the substitution product of $[PtI(dien)]^+$ with cystine at various pH and temperatures by ^{1}H NMR, elemental analysis (C, H, N) and IR. We have restricted this experiment in acidic medium, as at high pH, iodination of acetate, used for ionic strength maintenance (pH $\geq$ 3.95), occurred. We hope that this study will be helpful to understand in some measure the role of L-cystine in the reactions of $[PtI(dien)]^+$ in a biological domain along with a thorough light on the determination of condition for optimum product formation. This four biologically active product complexes, {$[\{Pt(dien)\}_2(S,S,cys)_2]^{4+}$ at $T \leq 313$ K of pH $\leq$ 3.30, $[\{Pt(dien)\}_2(S,S,cys)]^{4+}$ at $T \geq 318$ K of pH $\leq$ 3.30, $[\{Pt(dien)\}_2(N,S,cys)_2]^{2+}$ at $T \leq 313$ K of pH $\geq$ 3.95 and $[\{Pt(dien)\}_2(N,S,cys)]^{3+}$ at $T \geq 318$ K of pH $\geq$ 3.95}, might play some important role in pharmaceutical activity by this reaction at various conditions.

2. Results and discussion

2.1. *Reaction products*

The products are obtained by mixing $[PtI(dien)]^+$ + KI and cystine in 1:10 molar ratio at pH 2.30, 3.30 and 3.95. For ^{1}H NMR spectra, the mixtures are heated at 308 and 323 K for 24 h at each pH. Then, it is dried in silica gel desiccators. The white crystals are recrystallized from double-distilled water by filtering at room temperature. White crystals of irregular shape are found on drying in desiccators. The products are highly hygroscopic in nature.

2.2. *IR spectrometry analysis*

The spectra of Pt-complex with cystine at pH 2.30, 3.30 and 3.95 are interpreted for product identification. Figures S1–S3 are published as supporting materials.

At pH 3.95, Figure S1, NH asymmetric and symmetric stretching of cystine shifted from 3429 to 3553 cm^{-1} and 2096 to 2015 cm^{-1}, respectively. This is due to the bonding of Pt(II) with the NH_2 of cystine. The absence of a peak at 484 cm^{-1} pointed out that S−S symmetric stretching vibration

is disturbed and this peak is shifted to low at 472 cm^{-1}. This revealed that one Pt(II) formed a bond with L-cystine through one of the S−S bonds of cystine. At 512 cm^{-1}, a peak appeared due to the coordination between Pt(dien) and the NH_2 of cystine (*7–9*). Peaks at 628, 813 and 939 cm^{-1} are due to CH_2 rocking of the unsymmetrical arrangement of dien. The C−N stretching vibration of cystine shifted from 1043 to 1004 cm^{-1}. This also points out the formation of a Pt–N bond of cystine. The C−C (*31*) stretching vibration and CH_2–CO deformation vibration (*31*) of cystine remained intact at 1091, 1114, 1145 and 1411–1415 cm^{-1}, respectively, in the complex. The stretching vibration of COO^- (*31*) shifted from 1489 to 1455 cm^{-1} in the complex due to COOK formation. The C=O anti-symmetric stretching vibration remained intact in complex with cystine at 1591 cm^{-1} (*21*).

At pH 2.30 and 3.30, Figures S2 and S3, peaks at 626, 820 and 941 cm^{-1} are assigned to the CH_2 rocking of the unsymmetrical arrangement of dien. The CH_2–CO deformation vibration and stretching of COO^- on cystine remained intact at 1410 and 1500 cm^{-1}, respectively (*31*). The C−C stretching vibration shifted to high from 1090 to 1103 cm^{-1}. At pH 2.30, the S−S symmetric stretching vibration remained absent. This peak shifted to low at 468 cm^{-1} from 484 cm^{-1}. This reveals the formation of a Pt−S bond. This bonding confirmed the shift of C−S stretching vibration (*31*) from 675 to 720 cm^{-1}. The stretching vibration of NH_2 in cystine shifted from 2096 to low at 2020 cm^{-1}. This may be due to $–NH_3I^-$ but the Pt−N bond is ruled out due to the absence at 512 cm^{-1}. A peak at 3014 cm^{-1} is found due to CH broadband stretching at both pH.

2.3. *^{1}H NMR spectroscopy analysis*

This product of the mixture is freely soluble in D_2O solvents. Hence, it is readily characterized by ^{1}H NMR spectroscopy. Table 1 shows the ^{1}H NMR data at pH 2.30, 3.30 and 3.95 at temperatures 308 and 323 K. Figures S4–S9 are published as supporting materials.

At pH 2.30, ^{1}H NMR peaks (at temperature 308 K, Figure S4) appeared at δ (ppm): 1.25, 4.20 and 5.30 {(broad each), CH_2 (dien)}, 2.70–3.00 {triplet, CH (cystine), $J_{HH} = 50$ Hz} and 4.60–4.80 {doublet, CH_2 (cystine), $J_{HH} = 50$ Hz}. In this case, the H_α of CH in cystine is very pH-sensitive (*32*). The three ^{1}H NMR broad signals for the CH_2 of dien was an indication for unboltedness at NH_2 point. The easy displacement of amine (NH_2) group of dien ligand is probably a consequence of steric strained on Pt^{II}(dien) complex. This facilitated for easy substitution by one of the S−S bonds of cystine at each Pt(II) center. The product structure is given in Figure 1. At a high temperature, 323 K (Figure S5), the cystine peaks shifted to the right. The ^{1}H NMR peaks appeared at δ (ppm): 1.5 {triplet, CH_2 (dien)} and 2.40 {triplet, CH_2 (dien)}, 2.80–3.20 {CH (cystine)} and 4.60–4.80 {doublet, CH_2 (cystine)}. The two triplets for CH_2 of dien confirmed the existence of ring closure. As a result, one cystine attached with two Pt(II) centers through an S−S bond. The product structure is given in Figure 2.

At pH 3.30, ^{1}H NMR peaks (at temperature 308 K, Figure S6) appeared at δ (ppm): 1.30, 3.10 and 4.20{(broad peak), CH_2 (dien)}, 2.80–3.00 {multiplet, CH (cystine)} and 4.60–4.80 {doublet, CH_2 (cystine), $J_{HH} = 50$ Hz}. The three broad ^{1}H NMR signals for the CH_2 of dien was an indication for unboltedness at NH_2 point. This facilitated for easy substitution by one of the S−S bonds of cystine at each Pt(II) center. The product structure is given in Figure 1. The ^{1}H NMR peaks (at temperature 323 K, Figure S7) appeared at δ (ppm): 1.55 {triplet, CH_2 (dien)} and 2.45 {triplet, CH_2 (dien)}, 2.80–3.20 {multiplet, CH (cystine)} and 4.60–4.80 {doublet, CH_2 (cystine)}. The two triplets for the CH_2 of dien confirmed the existence of ring closing. As a result, one cystine attached with two Pt(II) centers through an S−S bond (Figure 2).

At pH 3.95, ^{1}H NMR peaks (at temperature 308 K, Figure S8) appeared at δ (ppm): 1.20–2.20 two ^{1}H NMR signals, 1.20–1.25 {triplet, CH_2 (dien) shielding due to NH_2 ring-opening site} and 2.20–2.25 {triplet, CH_2 (dien) deshielding due to NH_2 ring-closure site}, 5.25–5.75 {triplet,

Table 1. ^{1}H NMR data for product of reaction between $[PtI(dien)]^+$ with cystine at various pH at both 308 and 323 K.

pH	Complex	Temperature (K)	Solvent	Dien (δ, ppm)	Cystine (δ, ppm)	
				CH_2	CH_2	CH
3.95	$[\{Pt(dien)\}_2–\{N,S,cys\}_2]^{2+}$	308	D_2O	1.20–2.20 (2 ^{1}H NMR signal) {1.20–1.25 (triplet) and 2.20–2.25 (triplet)} and 5.25–5.75 (triplet)	4.75–4.80 (doublet) and 4.10–4.20 (doublet)	2.60–3.00 (multiplet) and 3.65–3.85 (triplet)
	$[\{Pt(dien)\}_2–(S,N,cys)]^{3+}$	323	D_2O	1.40–1.50 (triplet) & 2.40 (triplet)	4.10–4.20 (doublet) & 4.80 (broad peak)	2.80–3.10 (multiplet) & 3.90–4.00 (triplet)
3.30	$[\{Pt(dien)\}_2–\{S,S,cys\}_2]^{4+}$	308	D_2O	1.30, 3.10 and 4.20 (3 ^{1}H NMR broad signals)	4.60–4.80 (doublet)	2.80–3.00 (multiplet)
	$[\{Pt(dien)\}_2–\{S,S,cys\}]^{4+}$	323	D_2O	1.55 (triplet) and 2.45 (triplet)	4.60–4.80 (doublet)	2.80–3.20 (triplet)
2.30	$[\{Pt(dien)\}_2–\{S,S,cys\}_2]^{4+}$	308	D_2O	1.25, 4.20 and 5.30 (3 ^{1}H NMR broad signals)	4.60–4.80 (doublet)	2.70–3.00 (triplet)
	$[\{Pt(dien)\}_2–\{S,S,cys\}]^{4+}$	323	D_2O	1.50 (triplet) and 2.40 (triplet)	4.60–4.80 (doublet)	2.80–3.20 (triplet)

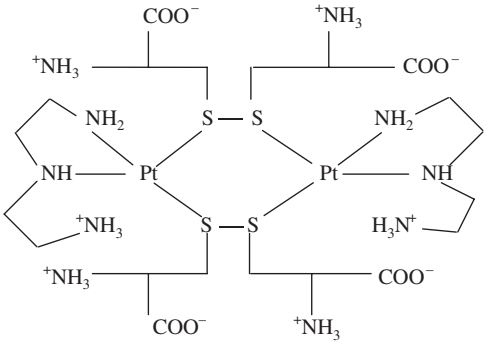

Figure 1. Structure of $[\{Pt(dien)\}_2(cys)_2]^{4+}$ at pH = 2.30 and 3.30 at 308 K.

CH_2 (dien)} which indicated that the ring opened at the –NH_2 site, 2.60–3.00 {multiplet, CH (cystine) shielding due to N non-bonding}, 3.65–3.85 {triplet, CH (cystine) deshielding due to N bond}, 4.80, 4.70 {doublet, CH_2 (cystine) deshielding due to S bond, $J_{HH} = 50$ Hz} and 4.10–4.20{doublet, CH_2 (cystine) shielding due to non-bonded S}. This indicated that cystine acts as a bidentate ligand through S and N donor atoms. Two cystine molecules attached with two Pt(II) centers. The product structure is given in Figure 3. At a high temperature, 323 K (Figure S9),

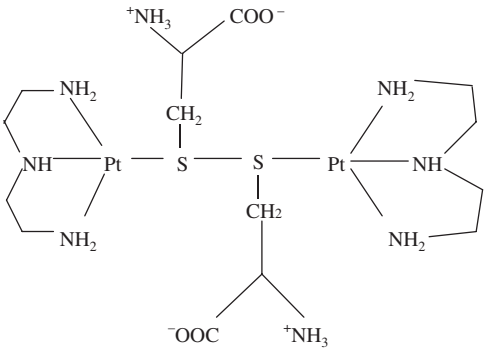

Figure 2. Structure of $[\{Pt(dien)\}_2(cys)]^{4+}$ at pH = 2.30–3.30 at 323 K.

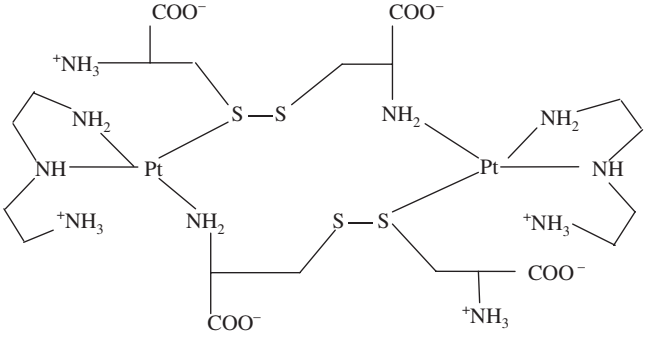

Figure 3. Structure of $[\{Pt(dien)\}_2(cys)_2]^{4+}$ at pH = 3.95 at 308 K.

^{1}H NMR peaks appeared at δ (ppm): 1.40–1.50 {triplet, CH_2 (dien)}, 2.40 {triplet, CH_2 (dien)}, 2.80–3.10 {multiplet, CH (cystine)}, 3.90–4.00 {triplet, CH (cystine)} and 4.10–4.20 {doublet, CH_2 (cystine)} 4.80 {broad peak, CH_2 (cystine)}. The two triplet peaks for CH_2 of dien confirmed the presence of the ring closure of dien in complex. Two ^{1}H NMR signals for CH_2 and CH groups indicated that cystine acts as a bidentate ligand. Here one cystine molecule attached with one Pt(II) center. The product structure is given in Figure 4.

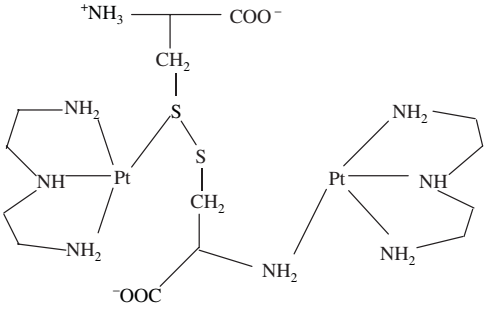

Figure 4. Structure of $[\{Pt(dien)\}_2cys]^{4+}$ at 323 K at pH 3.95.

2.4. *C, H and N analysis*

Empirical formula: $\{Pt_2S_4N_{10}O_8C_{20}H_{50}\}$ at 308 K at pH 3.30; cacld. C, 22.30%; N, 13.01%; H, 4.64%; found C, 22.1%; N, 12.9%; H, 4.92%; at 323 K at pH 3.30 empirical formula: $\{Pt_2S_2N_8O_4C_{14}H_{38}\}$; cacld. C, 18.66%; N, 12.44%; H, 4.22%; found C, 18.4%; N, 12.3%; H, 4.4%.

3. Kinetic analysis

The contribution of overall kinetics from possible reaction paths between $[PtI(dien)]^+$ complex with cystine is studied at different $[H^+]$. The kinetic results of second-order rate constant are tabulated using linear plots of equations having $Y = mX + C$ by plotting k_{obs}^{-1} *vs.* [L-cystine]$^{-1}$ for product formation and reversible and forward rate constants under $[PtI(dien)^+] = 1.0 \times 10^{-4}$, $I = 1.0 \times 10^{-1}$, [cystine] $= (1.0 - 3.0) \times 10^{-3}$ mol dm^{-3} and [KI] = 0.02 mM at pH 2.30–4.45 in the temperature range of 298–323 K.

3.1. *Effect of $[H^+]$*

3.1.1. *Forward reaction*

The pseudo-first-order rate constants (k_{obs}, s^{-1}) turned optimum at pH = 2.64 in comparison with pH 2.30 and 3.30. At $T \geq 318$ K, this might be due to the less bulky character of one cystine molecule $[\{Pt(dien)\}_2(S,S,cys)]^{4+}$ coordinating to two Pt(II) centers. At this pH ranges, the first-order product rate constant (k_{os}, $1.71 \times 10^{-3} \pm 0.68$ s^{-1}) turned optimum at pH 3.30 at 323 K. At $T \leq 313$ K, k_{obs} (s^{-1}) values decreased at high pH. At high pH, k_{obs} dropped off owing to the decrease in the activity of the S−S bond in cystine and bulky characters increased in the formation of products $[\{Pt(dien)\}_2(S,S,cys)_2]^{4+}$ by two cystine molecules with two Pt(II) centers (Scheme 1). The first-order product rate constants (k_{os}, s^{-1}) increased with an increase in pH from 2.64 to 3.30. The pseudo-first-order rate constant (k_{obs}, 7.06×10^{-4} s^{-1}), turned optimum at pH = 2.64 on 323 K having [cystine] $= 3.0 \times 10^{-3}$ mol dm^{-3}. The bulky character due to cystine, comparing product formation rate constant k_{os}, increased with an increase in $[H^+]$ by a factor of 1.15 times than that at pH 2.64 at $T \geq 318$ K. Between this pH range and $T \leq 313$ K, this bulky character is found almost constant with $[H^+]$.

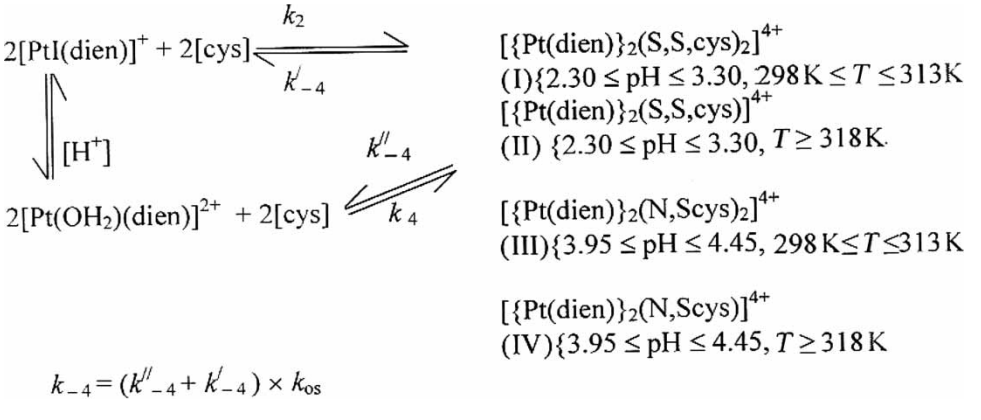

Scheme 1. Reaction of $[PtI(dien)]^+$ with cystine at various temperatures (298–323 K) and pH (2.30–4.45).

As far as second-order rate constants, k_4 ($M^{-1}\,s^{-1}$), are concerned, these rate constants decreased with the decrease in $[H^+]$ from pH 2.30 to 3.30. It is observed that, in the presence of I^-, $k_4(M^{-1}\,s^{-1})$ was greater than $[PtI(dien)]^+$ (28), $k_2 = 5.07 \pm 0.06 \times 10^{-1}$, pH = 2.30). From this, it is concluded that I^- facilitated the removal of the coordinate ligand. At this pH ranges, aqua Pt(II), $[Pt(dien)(OH_2)]^{2+}$, is more stable. The formation of the iodido complex decreased with the decrease in $[H^+]$. An intermediate product, $Pt(dien)(OH_2)I_2$, was formed through iodination by $[I^-]^*$ at $T \leq 313$ K. While at $T \geq 318$ K, the formation of the iodido complex increased with the decrease in $[H^+]$ and turned optimum ($k_{-1} = (36.7 \pm 2.97) \times 10^{-4}\,s^{-1}$) at 323 K at pH 3.30 when compared between pH 2.64 and 3.30. At pH 2.30–3.30 and $T \leq 313$ K, the rate of iodination of the aqua Pt(II) complex decreased with the decrease in $[H^+]$. At $T \geq 318$ K, the rate of iodination increased from pH 2.30 to 2.64 and decreased at pH 3.30 (Scheme 2). The first-order rate constant, $k_1 = (11.10 \pm 0.39) \times 10^{-4}\,s^{-1}$, turned optimum at pH 2.64 and 323 K.

As far as N, S and donor atoms of cystine are concerned, *i.e.* at pH $\geq$ 3.95, pseudo-first-order rate constants (k_{obs}, s^{-1}) increased. The pseudo-first-order rate constant (k_{obs}, $3.00 \times 10^{-4}\,s^{-1}$) turned optimum at pH = 4.45 at 323 K with [cystine] $= 3.0 \times 10^{-3}$ mol dm^{-3}. The first-order product rate constants (k_{os}, s^{-1}) increased from pH 3.95 to 4.45 and turned optimum (k_{os}, $2.32 \pm 0.35 \times 10^{-3}\,s^{-1}$) at 323 K at pH 4.45. At pH $\geq$ 3.95, the amine group of cystine is found to be apparently more reactive than the disulfide bond of cystine (*32*). At pH $\geq$ 3.95 and 298 K $\leq T \leq$ 323 K, it was found that k_{os} (4.45)/k_{os} (3.95) was greater than 1.33. This indicated that, along with cystine, the formation of aqua Pt(II) played a major role in first-order product rate constants of k_{os}.

In the case of $[PtX(dien)]^+$ (X = Br (*33*), Cl) complexes, the intermediate product $[Pt(dien)(OH_2)]^{2+}$ reacted faster with different ligands (pyridine, SCN^-, etc.). Here also the intermediate product, $Pt(dien)(OH_2)I_2$, reacted faster (k_4, $M^{-1}\,s^{-1}$) (Table 2) with cystine than direct substitution, k_2 ($M^{-1}\,s^{-1}$), at all examined pH. The second-order rate constants, k_2 ($M^{-1}\,s^{-1}$), increased with the increase in pH owing to the decrease in the formation of an aqua complex. It is evidenced that at low pH, the aqua complex is found to be more stable or it suppressed the formation of aqua complex in the presence of KI salt (*34*). Iodide ion facilitated the removal of coordinated I^- ligand from the complex. The second-order rate constants, k_2 ($M^{-1}\,s^{-1}$) (Table S1), turned optimum $(2.311 \pm 0.04)\,M^{-1}\,s^{-1}$, at pH = 4.45. Table S1 is published as a supporting material.

From pH 3.95 to 4.45, these second-order rate constants increased with the decrease in $[H^+]$ and turned optimum, $k_4 = 3.57 \pm 0.08\,M^{-1}\,s^{-1}$, at pH 4.45. At pH $\geq$ 3.95, the aqua ligand of $[Pt(dien)(OH_2)]^{2+}$ complex is more labile and is easily substituted by cystine to form product of species III and IV. On iodination by $[I^-]^*$, the intermediate product, $Pt(dien)(OH_2)I_2$, converted to the $[PtI(dien)]^+$ complex (Scheme 3). The rate of formation, k_{-1} (s^{-1}), of the iodido complex

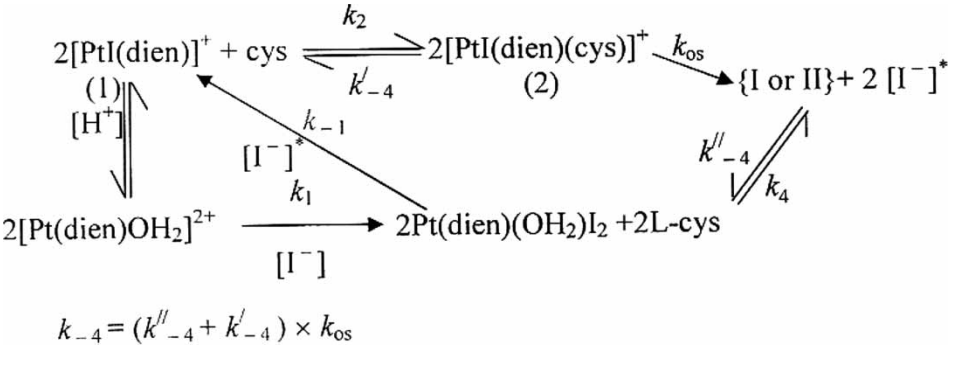

Scheme 2. Reaction of $[PtI(dien)]^+$ with cystine at various temperatures (298–323 K) and pH (2.30–3.30).

Table 2. First-order rate constants (k_1, s^{-1}), second-order rate constants (k_4, $M^{-1}\,s^{-1}$) and activation parameters for substitution reactions of mono functional Pt(II) complex with L-cystine in 0.10 M $NaClO_4$; $[Pt^{II}] = 1.0 \times 10^{-4}$ mol dm^{-3}; between 298 K $\leq T \leq$ 323 K under 2.30 $\leq$ pH $\leq$ 4.45.

Sl. No.	pH	Temperature (K)	$k_1 \times 10^4$ (s^{-1})	k_4 ($M^{-1}\,s^{-1}$)	$\Delta H^{\#}$ (kJ mol^{-1})	$\Delta S^{\#}$ ($JK^{-1}\,mol^{-1}$)	Ea (kJ mol^{-1})
1	2.30	298	1.52 ± 0.05	3.75 ± 0.03	31 ± 1	-175 ± 3	33 ± 0.73
		303	2.14 ± 0.06				
		308	2.73 ± 0.07				
		313	3.45 ± 0.10				
		318	4.39 ± 0.12				
		323	4.80 ± 0.14				
2	2.64	298	0.68 ± 0.04	3.34 ± 0.04	91 ± 2	-26 ± 4	94 ± 1.28
		303	1.08 ± 0.03				
		308	1.70 ± 0.06				
		313	2.71 ± 0.09				
		318	5.53 ± 0.19				
		323	11.10 ± 0.39				
3	3.30	298	0.55 ± 0.02	2.26 ± 0.08	68 ± 1	-100 ± 3	71 ± 0.55
		303	0.87 ± 0.03				
		308	1.36 ± 0.06				
		313	2.12 ± 0.09				
		318	3.53 ± 0.14				
		323	4.89 ± 0.20				
4	3.95	298	0.13 ± 0.15	2.18 ± 0.06	76 ± 1	-79 ± 3	78 ± 0.73
		303	0.22 ± 0.35				
		308	0.36 ± 0.58				
		313	0.59 ± 0.09				
		318	1.11 ± 0.18				
		323	1.41 ± 0.22				
5	4.45	298	0.27 ± 0.04	3.57 ± 0.08	66 ± 2	-105 ± 5	68 ± 1.71
		303	0.46 ± 0.07				
		308	0.79 ± 0.12				
		313	1.31 ± 0.20				
		318	1.85 ± 0.28				
		323	2.60 ± 0.38				

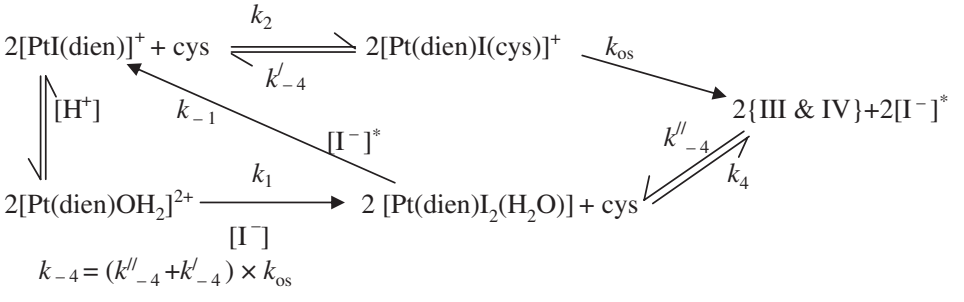

Scheme 3. Reaction of $[PtI(dien)]^+$ with cystine at various temperatures (298–323 K) and pH $\geq$ 3.95.

from the intermediate product, $Pt(dien)(OH_2)I_2$, increased with the decrease in $[H^+]$ and turned optimum, $k_{-1} = (8.93 \pm 0.15) \times 10^{-4}\,s^{-1}$, at pH 4.45 at 323 K. At these pH ranges, iodination of aqua Pt(II) complex to the intermediate product, $Pt(dien)(OH_2)I_2$, increased with the decrease in $[H^+]$ and turned optimum, $k_1 = (2.60 \pm 0.38) \times 10^{-4}\,s^{-1}$, at pH 4.45 at 323 K. As $k_{os} > k_1$ (Table 2 and Table S1), the liberated $[I^-]^*$ reacted with the intermediate product to form the $[PtI(dien)]^+$ complex (Schemes 2 and 3) at all $[H^+]$. Hence, the square planar geometry

converted to a five-member trigonal bipyramidal geometry. This reacted with cystine through the ring opening of dien (at low temperatures, both from IR and ^{1}H NMR) and ring closure at high temperatures to form the product as shown in Scheme 1.

3.1.2. *Reversible reaction*

Under the same experimental conditions of pseudo-first-order as above, the increase in pH from 2.30 to 3.30, the pseudo-first-order reversible rate constants ($k_{obs(r)}$, s^{-1}) for reversible reactions decreased except at $T \geq 313$ K at pH 3.30. At pH 3.30 and $T \geq 313$ K, these rate constants ($k_{obs(r)}$, s^{-1}) were larger than that at pH 2.64. This might be due to the partial formation of the Pt−S bond in the transition state. The pseudo-first-order rate constant, $k_{obs(r)}$ (4.69×10^{-3} s^{-1}), turned optimum at 323 K at pH 3.30 with [cystine] $= 1.0 \times 10^{-3}$ mol dm^{-3}. The second-order reversible rate constant ($k_{-4} = (6.56 \pm 0.08) \times 10^{-3}$ M^{-1} s^{-1}) turned optimum at pH 2.64. The first-order reversible rate constants (k_{-1}, s^{-1}) and second-order reversible rate constants (k_{-4}, M^{-1} s^{-1}) of reversible reactions are summarized in Table S2. Table S2 is published as a supporting material.

The pseudo-first-order reversible rate constants ($k_{obs(r)}$, s^{-1}) of reversible reactions increased with the increase in pH from 3.95 to 4.45. At these pH ranges, the second-order reversible rate constants (k_{-4}, M^{-1} s^{-1}) increased with the increase in pH and turned optimum, $(5.60 \pm 0.07) \times 10^{-3}$ M^{-1} s^{-1}, at pH 4.45.

3.1.3. *Product formation*

With the increase in pH from 2.30 to 3.30, the pseudo-first-order product rate constants ($k_{obs(p)}$, s^{-1}) increased. The pseudo-first-order product order rate constant ($k_{obs(p)} = 2.54 \times 10^{-3}$ s^{-1}) turned optimum at pH = 3.30 at 323 K with [cystine] $= 1.0 \times 10^{-3}$ mol dm^{-3}.

In the case of pH $\geq$ 3.95, the pseudo-first-order product rate constants ($k_{obs(p)}$, s^{-1}) increased with the increase in pH and conquered optimum at pH = 4.45 at 323 K ($k_{obs(p)} = 2.81 \times 10^{-3}$ s^{-1}) with [cystine] $= 1.0 \times 10^{-3}$ mol dm^{-3}. Products (III) and (IV) of Scheme 1 might be obtained by replacing two I^- ions by an ammonium moiety and one aqua by the S−S of cystine as shown in Schemes 2 and 3. It is seen that more products are obtained by the direct substitution of I^- at pH 4.45 at 323 K. This is observed due to the suppression of spontaneous solvolysis (*32*) reaction for the formation of the aqua complex by iodide ions.

3.2. *Effect of temperature*

The reaction is studied at five different temperatures with various [ligand] and pH. With the increase in temperatures, the pseudo-first-order rate constants for forward reactions, product formations and reversible reactions increased at all pH. The first-order rate constants for forward reaction, product formations and reversible reactions increased with the increase in temperature at all pH. Activation parameters are computed using a weighted program of the Eyring equation. The significantly negative entropy at pH = 4.45, 3.95, 3.30, 2.64 and 2.30 ($\Delta S^{\#} = -105 \pm 5$, -79 ± 3, -100 ± 3, -26 ± 4 and -175 ± 3 JK^{-1} mol^{-1}, respectively) of activation for the forward reaction suggested that the activation process in the present systems is dominated by bond making. However, it is indicated that the substitution reaction follows an associative A or Ia mode of activation (*33*). These data may suggest that in the case of L-cystine, a trigonal bipyramidal transition state is probably formed by hydrogen bonding between the entering ligand and the leaving water molecule of both $[Pt(dien)(H_2O)]^{2+}$ which did not stabilize.

3.3. *Steric factor*

In order to know whether steric effect is caused by unsymmetrical dien (*35*) of $[PtI(dien)]^+$ or cystine, the second-order rate constants ($k_{obs(2)}$, $M^{-1}\,s^{-1}$) are calculated with the variation of $(3.0 \times 10^{-3}\,mol\,dm^{-3}) \geq [PtI(dien)^+] \geq (1.0 \times 10^{-3}\,mol\,dm^{-3})$ at fixed $[cystine]_T = 1.0 \times 10^{-4}\,mol\,dm^{-3}$ at pH $\geq$ 3.95. It was found, like cystine, that the k_{obs} *vs.* Pt^{II} graph was not linear. A parabolic curve was observed at higher $[PtI(dien)^+]$ but k_{obs}^{-1} *vs.* $[PtI(dien)^+]^{-1}$ was linear. Hence, the cystine and dien ligands of $[PtI(dien)]^+$ were responsible for the steric effect.

4. Mechanism

The coordinated iodido molecule on Pt^{II} centers is easily substituted by pyridine than other nucleophilic leaving groups such as N_3^-, SCN^-, CN^-, etc., due to their labile nature (*36*). The disulfide moiety of cystine is targeted by the Pt^{II} center at $2.30 \leq pH \leq 3.30$. This is observed by the time-resolved UV–visible electronic spectrum ($\lambda = 290$ nm). The ammonium moiety of cystine is targeted by the Pt^{II} center at $3.95 \leq pH \leq 4.45$. This is observed by the time-resolved UV–visible electronic spectrum ($\lambda = 300$ nm). The k_{obs} values of forward reaction, product formation and reversible reaction, E1–E6, are published as supporting materials.

The simplest mechanism described by Scheme 1 by taking into account the protolysis of the incoming ligands and the $[Pt\,I(dien)]^+$ complex in the presence of KI at all temperatures is given below. This mechanism is based on the formation of products (*28b*), characterized by IR and ^1H NMR spectra, as shown in Schemes 1–3.

$$\frac{d[product]}{dt} = k_{os}2[Pt(dien)I(cys)]^+ + k_4 2[Pt(dien)I_2(OH_2)][cys]^2 - k_{-4}^{//}[I^-]^{2*}[product]$$

$$\frac{d}{dt}[product] = k_{os}\left\{\frac{k_2[Pt\,I(dien)]^+[cys]}{k_{-4}^{/}k_{-4}^{//}[I^-]^{2*}}\right\} + k_4\left\{\frac{k_1 2[Pt(dien)(OH_2)]^{2+}[I^-] + k_{-4}^{//}[I^-]^{2*}}{k_{-1}[I^-]^*[cys]^2 k_{-4}^{//}[I^-]^{2*}}\right\}$$

5. Experimental

The compound [PtI(dien)]I was synthesized according to the literature (*37*). Chemical analysis, UV–visible and ^1H NMR spectroscopic data were in good agreement with those obtained previously (*7–9*). It was known that the perchlorate ion does not coordinate with Pt(II) in aqueous solution (*38*). So, the kinetics of complex formation reactions was studied in the perchlorate medium at pH $\leq$ 3.30. Also, it was found that sodium acetate did not react with Pt(II) in the aqueous solution at pH $\geq$ 3.95. The ionic strength of the solution was adjusted to 0.1 M with $NaClO_4$ (at pH $\leq$ 3.30) and CH_3COONa (at pH $\geq$ 3.95). $NaClO_4$ was prepared by neutralizing $HClO_4$ with freshly prepared standardized stock solutions of NaOH in a water bath maintained at $\sim$ 343 K. While cooling, the crystals of $NaClO_4$ were obtained from which the appropriate concentration of the stock solution was prepared. The pH of the stock $NaClO_4$ solution ($1\,mol\,dm^{-3}$) was adjusted to 6.0 and estimated for Na^+ by a combined ion exchange alkalimetric procedure. Analar-grade chemicals (E-Merck) were used for all kinetic studies. L-Cystine was prepared without further purification shortly before use. The pH of the stock solution for both $[PtI(dien)]^+$ with KI and cystine was maintained shortly before experimentation. Both the complex and the ligand were found to be stable under experimental conditions. As the [PtI(dien)]I complex alone was not readily soluble in water, for solubility it was kept with KI salt of 0.02 mM for 10 days. For cystine solubility in experimental conditions, first the quantity of cystine was soluble in a minimum amount of $HClO_4$ acid was calculated. Then, the desired concentration was prepared by the

addition of double-distilled water. Highly purified, deionized water was used in all solutions. The second distillation was made from alkaline $KMnO_4$ using an all-glass distillation apparatus.

5.1. *Physical measurements*

The pH measurement was performed using a Nucleonix type DP 301 digital pH meter equipped with a combination of glass-Ag/AgCl, Cl^- (3 mol dm^{-3} NaCl) electrode. It was calibrated with standard buffers of pH 4.0, 7.0 and 9.0 (Merck). The pH data (*i.e.* meter readings) at pH < 7 were converted to $-\log [H^+]$ by a calibration curve as described earlier (*20*). UV–visible spectra were recorded with a Cecil UK model CE-7200 UV–visible spectrophotometer using cell block housing a pair of 10 mm Quartz Suprasil cells. ^{1}H NMR spectra were recorded at temperatures of 308 and 323 K at pH 3.95 and 2.35, 3.30 at 308 K by a 500 MHz spectrometer model: UNITY–400, Varian, Switzerland with D_2O used as a solvent in IICT (Indian Institute of Chemical Technology), Hyderabad. IR spectra were recorded at room temperature with pH of 2.30, 3.30 and 3.95 with Shimadzu 8300 FTIR spectrometer. The elemental analysis (C, H, N) was carried out with Perkin Elmer 240C element analyzer at IIT Madras.

5.2. *Kinetic measurements*

The reactions of the complex were monitored under pseudo-first order conditions as well as first-order of the complex and cystine as follows. All kinetics reactions were inspected in aqueous perchlorate/acetate medium at different temperatures and $[H^+]$. All activation parameters such as $\Delta H^{\#}$ and $\Delta S^{\#}$ were determined by the Eyring equation from temperature variation experiments. The activation energy was determined from the Arrhenius equation. A constant temperature was maintained by an external circulating thermostat ($\pm$273.01 K) connected to a Peltier. The reaction of cystine and $[PtI(dien)]^+$ was studied using the ligand in excess ($\geq$10-fold). All reactions were studied in the perchlorate/acetate medium with the total ionic strength of 1.0×10^{-1} mol dm^{-3} with different temperatures (298, 303, 308, 313, 318 and 323 K) and $[H^+]$. At high pH $\geq$ 3.95, the ionic strength was maintained by sodium acetate due to the indiscretion of pH during reaction time by using $NaClO_4$. The ionic strength as well as pH-adjusted solution of the reaction mixture was thermally equilibrated in a 10 cm^3 measuring flask and then a known volume (1 cm^3) of the stock complex solution was added. This reaction mixture was quickly (ca. $\leq$ 10 s) transferred to the cell placed in the thermostated cellblock of the spectrophotometer. The reactions were followed for at least 75% of the reaction at suitable wavelengths where respective absorbance changes were largest than that obtained from repetitive runs at different time intervals of various pH. Spectral changes resulting from the mixing of the complex and the peptide solution were recorded between 250 and 410 nm. At 4.50 $\geq$ pH $\geq$ 3.95, the repetitive spectral scans for the reaction mixture of $[PtI(dien)]^+$ and L-cystine displayed a steady decrease in absorbance with time at 300 and 290 nm at 2.30 $\leq$ pH $\leq$ 3.30 against 408 nm (before reaction). The progress of the reaction was monitored at a pre-selected wavelength by recording absorbance with time against the solvent (water). The [cystine] was varied as 1.0–3.0 $\times 10^{-3}$ mol dm^{-3}. $[PtI(dien)^+]$ was kept at 1.0×10^{-4} mol dm^{-3} throughout the pseudo-first-order experiment. Linear kinetic traces were collected in all cases from absorbance (A_t)–time (t, s) data and the pseudo-first-order rate constants (k_{obs}, s^{-1}) were evaluated from the slope by fitting in the equation $Y = m X + C$ by plotting $\ln (A_t - A_\infty)$ *vs.* time (t, min). The pseudo-first-order product rate constants (*28b*) ($k_{obs(p)}$, s^{-1}), were observed by plotting $\ln(A_t - A_o)$ *vs.* time (t, s). Similarly, the pseudo-first-order reverse rate constants ($k_{obs(r)}$, s^{-1}) were evaluated by plotting $\ln\{(A_t - A_o)/(A_o - A_{50})\}$ *vs.* time (t, s) (where A_t, A_o, A_{75} and A_∞ are the absorbances at different time intervals, initial absorbance, absorbance at 75% of reaction and at final, respectively). The data fitting involved 50 data points in most cases. All calculations are made on a PC using linear and nonlinear least squares programs.

Acknowledgements

The author (T.S.) thanks Department of Chemistry, Utkal University, for providing support on this research work. The authors are thankful to the Pharmaceutical Department for providing IR spectra.

References

(1) Reedijk, J.; Teuben, M.J. *Cisplatin Chemistry and Biochemistry of Leading Anticancer Drugs*: Lippert, B., Ed.; Wiley-VCH: Zurich, 1999; pp 339–362.
(2) (a) Reedijk, J. *Chem. Rev.* **1999,** *99* (9), 2499–2510; (b) Wong, E.; Grandomenico, C.M. *Chem. Rev.* **1999,** *99* (9), 2451–2466; (c) Jamieson, E.R.; Lippard, S.J. *Chem. Rev*. **1999,** *99* (9), 2467–2498; (d) Fuertes, M.A.; Alonso, C.; Perez, J.M. *Chem. Rev*. **2003,** *103*, 645–662.
(3) Dedon, P.C.; Borch, R.F. *Biochem. Pharmacol*. **1987,** *36*, 1955–1964.
(4) Bodenner, D.L.; Dedon, P.C.; King, P.C.; Borch, R.F. *Cancer Res*. **1986,** *46*, 2745–2750.
(5) Daley-Yates, P.T.; McBrien, D.C.H. *Chem. Biol. Interact.* **1982,** *40*, 325–334.
(6) Guarino, A.M.; Miller, D.S.; Arnold, S.T.; Pritchard, J.B.; Davis, R.D.; Urbanek, M.A.; Miller, T.J.; Litterst, C.L. *Cancer Treat. Rep*. **1979,** *63*, 1475–1483.
(7) Soldatovic, T.; Bugarcic, Z.D. *J. Inorg. Biochem*. **2005,** *99*, 1472–1479.
(8) Petrovic, B.V.; Bugarcic, Z.D. *Aust. J. Chem*. **2005,** *58*, 544–550.
(9) Vasic, V.; Zivanovic, M.; Cakar, M.; Savic, J.; Nedeljkovic, J.; Bugarcic, Z.D. *J. Phys. Org. Chem*. **2005,** *18* (5), 441–447.
(10) Bugarcic, Z.D.; Heinemann, F.W.; van Eldik, R. *Dalton Trans*. **2004,** 279–286.
(11) Bugarcic, Z.D.; Soldatovic, T.; Jelic, R.; Alguero, B.; Grandas, A. *Dalton Trans*. **2004,** 3869–3877.
(12) Bugarcic, Z.D.; Jancic, D.; Shoukry, A.A.; Shoukry, M.M. *Monatsh. Chem*. **2004,** *135*, 151–160.
(13) Jakupec, M.A.; Galanski, M.; Keppler, B.K. *Rev. Physiol. Biochem. Pharmacol*. **2003,** *146*, 1–53.
(14) Yuhas, J.M.; Culo, F. *Cancer Treat. Rep*. **1980,** *64* (1), 57–64.
(15) Howell, S.B.; Taetle, R. *Cancer Treat. Rep*. **1980,** *64* (4–5), 611–616.
(16) Yuhas, J.M.; Spellman, J.M.; Jordan, A.W.; Pardini, M.C.; Afzal, S.M.J.; Culo, F. *Br. J. Cancer* **1980,** *42*, 574–585.
(17) Howell, S.B.; Pfeifle, C.E.; Wung, W.E.; Olshen, R.A. *Cancer Res*. **1983,** *43*, 1426–1431.
(18) Borch, R.F.; Pleasants, M.E. *Proc. Natl Acad. Sci. USA* **1979,** *76*, 6611–6614.
(19) Borch, R.F.; Katz, J.C.; Leider, P.H.; Pleasants, M.F. *Proc. Natl Acad. Sci. USA* **1980,** *77*, 5441–5444.
(20) (a) Irving, H.M.; Miles, M.G.; Pettit, L.D. *Anal. Chim. Acta* **1967,** *38*, 475–488; (b) Das, A.; Dash, A.C. *Dalton Trans.* **2000,** 1949–1958.
(21) Centeno, J.A.; Ishak, K.G.; Mullick, F.G.; Gahi, W.A.; O'Leary, T.J. *Appl. Spectrosc*. **1994,** *48*, 569–572.
(22) Oehlsen, M.E.; Qu, Y.; Farrell, N. *Inorg. Chem.* **2003,** *42* (18), 5498–5506.
(23) Sharma, K.; Swami, M.; Singh, R.; Fahmi, N.; Singh, R.V. *Phosphorous Sulfur Silicon Relat. Elem.* **2009,** *184* (8), 1964–1974.
(24) Cleare, M.J.; Hoeschele, J.D. *Bioinorg. Chem*. **1973,** *2*, 187–210.
(25) Johnson, N.P.; Macquet, J.P.; Weibers, J.L.; Monsarrat, B. *Nuclic Acid Res.* **1982,** *10*, 5255–5271.
(26) Bugarcic, Z.D.; Leiehr, G.; van Eldik, R. *Dalton Trans*. **2002,** 951–956.
(27) Bugarcic, Z.D.; Leiehr, G.; van Eldik, R. *Dalton Trans*. **2002,** 2825–2830.
(28) (a) Baral, D.K.; Brahma, G.S.; Swain, T.; Sahu, M.; Mohanty, P. *J. Indian Chem. Soc*. **2006,** *83*, 131–134; (b) Swain, T.; Mohanty, P. *Aust. J. Chem*. **2009,** *62* (5), 493–500.
(29) (a) Read, J.F.; Bewick, S.A.; Graves, C.R.; Macpherson, J.M.; Salah, J.C.; Theriault, A.; Wyand, A.E.H. *Inorg. Chim. Acta* **2000,** *303*, 244–255; (b) Kembhavi, Md.S.R.; Panari, R.G.; Nandibewoor, S.T. *Inorg. React. Mech.* **1999,** *1*, 225; (c) Annapurna, N.; Kumar, A.K.; Vani, P.; Rao, G.N. *Trans. Met. Chem*. **2008,** *33*, 691–696; (d) Shaidarova, L.G.; Ziganshina, S.A.; Budnikov, G.K. *J. Anal. Chem*. **2003,** *58* (6), 577–582.
(30) Larkworthy, L.F.; Turnbull, M.H.; Yavari, A. *Inorg. Chim. Acta*. **1985,** *106*, 109–114.
(31) Ramachandran, E.; Natarajan, S. *Crystal Res. Technol*. **2004,** *39* (4), 308–312.
(32) Nagy, P.; Ashby, M.T. *Chem. Res. Toxicol*. **2005,** *18*, 919–923.
(33) Gray, H.B.; Olcott, R.J. *Inorg. Chem*. **1962,** *1*, 481–485.
(34) Rosic, J.; Petrovic, B.; Djuran, M.I.; Bugarcic, Z.D. *Monatsh. Chem.* **2006,** *138*, 1–11.
(35) Basolo, F.; Chatt, J.; Gray, H.B.; Pearson, R.G.; Shaw, B.L. *Dalton Trans*. **1961,** 2207–2215.
(36) Basolo, F.; Gray, H.B.; Pearson, R.G. *J. Am. Chem. Soc*. **1960,** *82*, 4200–4203.
(37) Annibale, G.; Brandolisio, M.; Pitteri, B. *Polyhedron* **1995,** *14*, 451–453.
(38) Appleton, T.G.; Hall, J.R.; Ralph, S.F.; Thompson, C.S.M. *Inorg. Chem*. **1984,** *23*, 3521–3525.